Microscopic theory of the martensitic transition in $Fe_{1-x}Ni_x$

E. Hoffmann, H. Herper, and P. Entel
Theoretische Tieftemperaturphysik and SFB 166, Universität-GH-Duisburg, W-4100 Duisburg 1, Germany

S. G. Mishra
Institute of Physics, Sachivalaya Marg, Bhubaneswar-751 005, Orissa, India

P. Mohn and K. Schwarz
Institut für Elektrochemie, Technische Universität Wien, A-1060 Wien, Austria
(Received 15 October 1992)

Fixed-spin-moment band-structure calculations of Fe_3Ni show that the face-centered-cubic structure is unstable with respect to small tetragonal distortions. Using the Bain transformation for the crossover from the fcc to the bcc structure, we show that the ground state of Fe_3Ni corresponds, in agreement with experiment, to the bcc structure, which is by 1.75 mRy/atom lower in energy than the fcc structure. The band structure of the nonmagnetic phase of fcc Fe_3Ni reveals Fermi-surface nesting, which can give rise to Kohn-like anomalies. This nesting behavior is very similar to what has recently been found in the nonmagnetic Ni_xAl_{1-x} compound [G. L. Zhao and B. N. Harmon, Phys. Rev. B **45**, 2818 (1992)]. We argue that this nesting behavior is one of the causes for the martensitic transition in Fe_3Ni. The change in the phonon-dispersion curves, which is connected with the formation of martensite, is evaluated by using the method of Varma and Weber [C. M. Varma and W. Weber, Phys. Rev. Lett. **39**, 1094 (1977)]. We find pronounced softening of the TA_2 shear mode for **q** in the [110] direction and a polarization vector along the [001] direction. The search for Invar anomalies in fcc Fe_3Ni has shown that there are two competing effects, of which one is connected with the structural change from the fcc to the bcc structure, and the other with the magnetovolume instability in the fcc structure, involving a transition from the low-moment (LM) to the high-moment (HM) state in a critical range of volumes. It is argued that in $Fe_{1-x}Ni_x$ and for $x > 0.65$ the gain in energy due to the formation of martensite is more favorable as compared to the gain in exchange energy from the LM→HM transition, whereas for $x < 0.65$ is it more favorable to form Invar.

I. INTRODUCTION

With a decrease in temperature Fe_3Ni undergoes a $\gamma \rightarrow \alpha$ transition at ≈ 700 K which is accompanied by onset of ferromagnetic order. This transition is of first order with an unusual broad temperature hysteresis curve. On the other hand, Fe_3Ni is close in concentration to the Invar region, where premartensitic behavior without a structural phase transition is observed. Therefore, this alloy is an ideal model system which allows us to study both, the formation of martensite and the study of Invar related effects. For recent reviews, in which the mutual interplay of lattice and electronic degrees of freedom in Invar systems is discussed in great detail, we refer to Ref. 1.

On the basis of band-structure calculations Invar related effects in the fcc structure of Fe_3Ni have recently been discussed in great detail.[2–6] Of particular interest is the observation that in the fcc structure two types of ferromagnetic solutions exist, low-moment (LM) solutions are found at low volumes, whereas high-moment (HM) solutions are found at high volumes.[2] In the HM ground state the occupation of strongly antibonding majority-spin bands is responsible for the HM and the large volume of the unit cell. The manifestation of the LM state is connected with charge transfer from these antibonding majority-spin bands to nonbonding minority-spin bands, which in turn causes the volume to shrink.[6] This kind of charge transfer also occurs with increasing temperature and decreasing exchange splitting. Therefore, Invar can be typified by stating that HM and LM solutions approach each other with increase in T, and that they finally merge at the Curie temperature T_c. This mechanism can be used to describe vanishing thermal expansion and other anomalies in Invar alloys.[2–6]

In this paper we focus on the $\gamma \rightarrow \alpha$ transition in Fe_3Ni and try to describe this transition in the frame of existing theories for the formation of martensite. To this we will briefly discuss a few theoretical concepts which are frequently used.

Many nonmagnetic intermetallic compounds undergo structural changes, usually from a less-closed-packed structure at high temperatures to a closed-packed structure at low temperatures (for example, from bcc at high T to fcc at low T). In many magnetic intermetallic compounds the opposite occurs. A well-known example for the latter case is the lattice deformation from fcc austenite to bct (bcc) martensite in steel ($Fe_{1-x}C_x$) with decreasing temperature. Bain's model for the formation of martensite in steel is displayed in Fig. 1, which shows a bct lattice delineated in the fcc austenite structure.[7] The bcc structure is then obtained by compressing the bct lat-

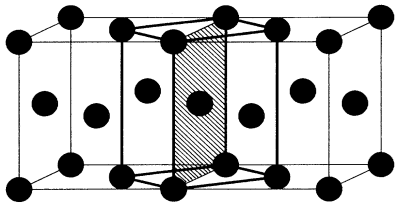

FIG. 1. Bain's 1924 model for the formation of martensite showing a bct lattice delineated in the fcc structure (Ref. 7). The bcc lattice is produced by an appropriate tetragonal deformation of the bct lattice.

tice. Other topological paths exist for the lattice deformation from fcc to bcc, for example, the principal uniform shear, $a_0/12[112]$ of every successive (111) plane (a_0 is the lattice constant of the fcc structure).[8]

In nonmagnetic intermetallics the formation of martensite is connected with the appearance of unusual properties, for example, a tweed precursor pattern, or an anomalous low [110] TA_2 branch with a dip at $\mathbf{q}\neq\mathbf{0}$, which depends strongly on temperature and composition. Different proposals for the microscopic origins of such structural transformations exist: that these are soft-mode transitions, that they are connected with the formation of a charge density wave (CDW) (i.e., with a Peierls instability), that singular Fermi-surface effects such as nesting play a dominant role in the transformations and precursors.[9] The following picture emerges from these discussions: Martensitic transformations are associated with large anharmonicities, they are displacive, diffusionless, and of first order. They cannot be described by a soft-mode theory (i.e., a structural transformation of second order). Most theoretical models are based on concepts such as large anharmonicity effects,[10] Fermi-surface nesting, and Kohn anomalies,[11,12] on Landau expansions,[13] and on spin-analog models.[14,15] While large anharmonicity effects are believed to be responsible for driving the martensitic transformation (which means that the atomic positions of the parent and the resultant structure are highly correlated, leading to anomalous temperature dependence of whole phonon branches), Kohn-like anomalies are thought to be responsible for the transition to an intermediate phase (precursor) and a resulting dip in the lower transverse phonon branch.

In this paper we show that fixed-spin-moment (FSM) band-structure calculations[16,17] can describe the $\gamma\rightarrow\alpha$ transition in the $Fe_{1-x}Ni_x$ system at zero temperature, provided the calculation is done under the constraint which keeps track of the correct volume change during the transition. This is described in Sec. II. In Sec. III we present calculations of phonon-dispersion curves which are renormalized by precursor effects. In Sec. IV we analyze the formation of martensite and of Invar in the $Fe_{1-x}Ni_x$ system by using a Ginzburg-Landau (GL) description with FSM data as input. Section V contains the summary and an outlook of future work.

II. THE $\gamma\rightarrow\alpha$ TRANSITION IN $Fe_{1-x}Ni_x$

The actual compound Fe_3Ni is disordered down to lowest temperatures making accurate first-principles calculations unfeasible. Therefore, we have used the easiest approach and considered ordered Fe_3Ni.

Figures 2(a) and 2(b) show the results of spin-polarized augmented-spherical-wave[18] band calculations (using the FSM procedure) of the total energy and of the average magnetic moment per atom of Fe_3Ni for the transition from the face-centered to the body-centered structure (Bain's model). We find that fcc and bcc states are separated by a tiny energy barrier of 0.25 mRy/atom and that the bcc structure is lower in energy by 1.75 mRy/atom. So the bcc structure is the ground-state structure of Fe_3Ni in agreement with experiment. Also the ground-state values of magnetic moment and Wigner-Seitz radius of the bcc structure compare well with experimental values. We expect that these results will not much change if, in addition, statistical disorder is taken into account.[19] Note that similar calculations of the energetics involved in the fcc-bcc lattice deformation along the tetragonal Bain-deformation path have recently been undertaken by Krasko and Olson for the case of iron.[20] They found that the ferromagnetic fcc phase corresponds to an enthalpy maximum, which means that the fcc phase is unstable with respect to a tetragonal deformation, and therefore cannot exist. This is very similar to our results for the case of Fe_3Ni. Note also that the difference of enthalpies found by Krasko and Olson for iron between the nonmagnetic fcc and the ferromagnetic bcc phase is of the order of 5 mRy for zero pressure. In intermetallic compounds such as Fe_3Ni, which are even more soft, we expect this energy difference to be smaller. Therefore, the calculated energy difference of 1.75 mRy for the case Fe_3Ni can be considered as a *good guess.*

In the actual calculations we have used the constraint that the next-nearest-neighbor distance between the Fe atoms does not change during the transformation. The resulting lattice constant of the bcc phase is $2a_0/\sqrt{3}$, where a_0 is the original fcc lattice constant. This constraint implies furthermore that we have always a closely packed structure at each step of the transformation. Therefore, we expect that the energy differences found

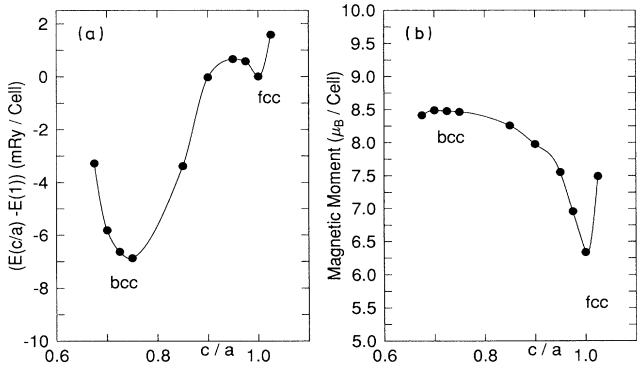

FIG. 2. (a) Fixed-spin-moment total energy of Fe_3Ni along the Bain path. fcc: $r_{WS}=2.60$ a.u., $M=1.58\mu_B$/atom. bcc: $r_{WS}=2.67$ a.u., $M=2.11\mu_B$/atom. (b) Change of the magnetic moment along the Bain path.

between undistorted and tetragonal distorted lattices are not too unreasonable, in spite of the atomic sphere approximation used in the calculation.

With respect to the Invar effect in fcc Fe_3Ni we have recently shown that the FSM calculations confirm Kaspar and Salahub's cluster calculations, according to which the Invar effect is a consequence of collective thermal excitations of electrons from the antibonding majority-spin level into the close in energy lying minority-spin level of nonbonding character,[21] which is equivalent to saying that the system undergoes a transition from the HM ground state to the LM state and then to the nonmagnetic (NM) state with increasing temperature.[6] The cooperative nature of this charge transfer is due to the coherent coupling of the electrons involved in local distortions, which do not cost much energy. The energy difference between the HM ground state and the excited LM state is of the order of 1 mRy/atom.

We now have the following energetic situation in Fe_3Ni. The ground state of Fe_3Ni corresponds to the bcc structure with a Wigner-Seitz radius of $r_{WS}=2.67$ a.u. and a magnetic moment of $M=2.11\mu_B$/atom. The excited state is then the ferromagnetic ground state of the fcc phase, which lies 1.75 mRy/atom higher in energy, with $r_{WS}=2.60$ a.u. and $M=1.58\mu_B$/atom. The next and overnext excited states are the LM and NM state of the fcc phase, which lie 2.75 mRy and 7.75 mRy above the ground-state energy of the bcc phase, respectively, while the NM state of the bcc structure lies ≈ 6 mRy above its ground-state value. Since the fcc LM state has only a very shallow local-energy minimum, which is washed out with increasing temperature, we expect the following finite-temperature scenario. With increasing temperature bcc Fe_3Ni will become nonmagnetic at $T\approx 6$ mRy$=970$ K and will simultaneously undergo a structural transformation to the close in energy lying nonmagnetic fcc state. The actually observed transition temperature for this process is lower, but we must bear in mind that these zero-temperature considerations do not take into account the impact of magnetic and structural fluctuations.

We believe that for the Invar composition $Fe_{0.65}Ni_{0.35}$ the situation will have changed. Now it is the fcc phase with a ferromagnetic ground state that has the lowest energy, and excited states are (due to statistical disorder) many close in energy lying states, which cover the whole range between the HM ground state and the high-temperature paramagnetic state. Yet it still does not cost much energy to make small tetragonal or shear distortions, which then are responsible for precursor effects in Invar. The nonmagnetic bcc state lies too high in energy to be of any importance and the system remains in the fcc structure up to the melting temperature. Supercell calculations for Fe_5Ni_3, which corresponds to $Fe_{0.625}Ni_{0.375}$, show that besides the HM ground state, there is only a single LM state (which lies only 0.3 mRy above the HM state).[22] However, we expect that disorder will smear out the shallow local-energy minimum of the LM state and will lead to many close in energy lying HM-LM states (this is a guess and will be checked by Korringa-Kohn-Rostoker coherent-potential-approximation calculations[19]).

III. FERMI-SURFACE NESTING AND KOHN-LIKE ANOMALIES IN Fe_3Ni

The actual martensitic transformation which takes place in Fe_3Ni is complex and involves, as discussed above, cooperative, rather than diffusive, large displacements of atoms. A true microscopic theory is not at hand. Yet several distinct concepts have proven to be quite successful.[9–15] In particular, there is the belief that phonons and strong anharmonic interactions are involved. Indeed, it seems that near all martensitic transformations the vibrational frequencies of a particular symmetry decrease. In cubic systems it is the TA_2 shear mode in the [110] direction and a polarization vector along $[1,\bar{1},0]$ (for bcc structures) and along [0,0,1] (for fcc structures) that are mostly affected.

Of interest is the recent observation that the phonon anomalies in the TA_2 branch of β-phase Ni_xAl_{1-x} alloys can be attributed to both strong electron-phonon interactions and Fermi-surface nesting.[11] If this turns out to be a common feature of martensitic transformations in nonmagnetic compounds, then the question is, whether this is also true for magnetic martensitic phase transitions in systems such as Fe_3Ni. As we will show, there is strong evidence from FSM energy-band calculations that this is so.

To this we have calculated the hypothetical band structure of the paramagnetic high-temperature phase of fcc Fe_3Ni shown in Fig. 3, which mimics the situation just before the simultaneous appearance of magnetism and martensite. One characteristic feature is that the related Fermi surface of two energy bands (bands 17 and 18) shows nesting behavior with nesting wave vectors $\mathbf{Q}_1=0.8[1,1,0]\pi/a_0$ and $\mathbf{Q}_2=0.6[1,1,0]\pi/a_0$ (see Fig. 4). FSM calculations of the generalized susceptibility show that this nesting behavior leads to a peak centered between $\mathbf{Q}_1$ and $\mathbf{Q}_2$ on top of a large background. This is shown in Fig. 5.

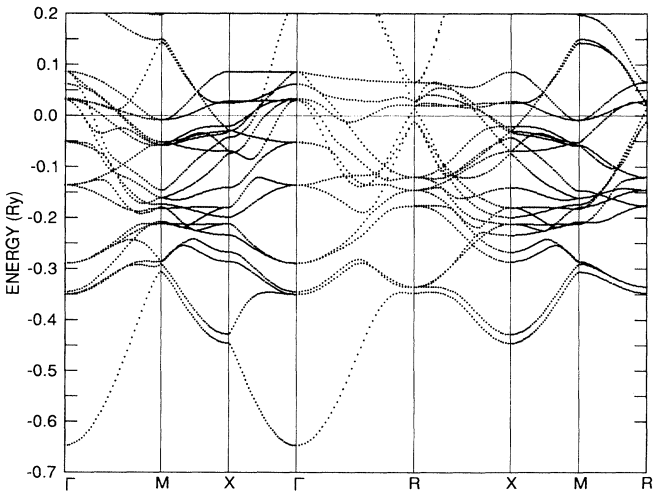

FIG. 3. Fixed-spin-moment band structure of fcc Fe_3Ni for $r_{WS}=2.60$ a.u. and $M=0$. Energies are relative to the Fermi energy.

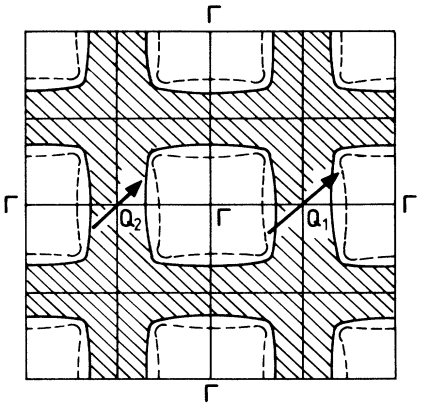

FIG. 4. The Fermi surface of two bands (band 17: dashed curve, band 18: solid curve) of nonmagnetic fcc Fe_3Ni ($r_{WS}=2.60$ a.u.).

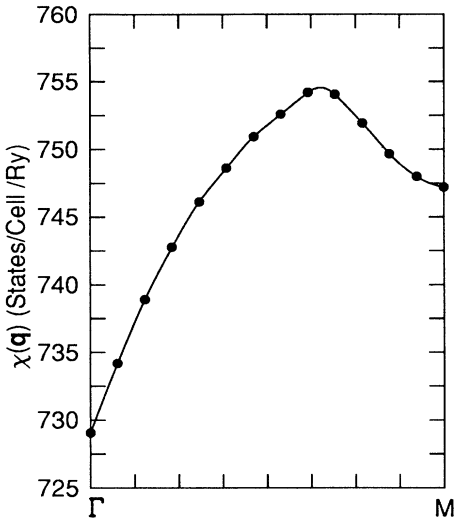

FIG. 5. Fixed-spin-moment results of the generalized susceptibility $\chi(\mathbf{q})$ along the [110] direction in fcc Fe_3Ni. Note the very large background.

It is known that such an enhanced susceptibility can lead to Kohn-like anomalies in the phonon spectrum. In order to check this, we have calculated the phonon-dispersion curves by using the method of Varma and Weber.[23] Varma and Weber have shown that the dynamical matrix $\mathcal{D}$ can be decomposed into $\mathcal{D}=\mathcal{D}_1+\mathcal{D}_2$, where $\mathcal{D}_1$ contains the short-range interactions, which in this work will be described by a Born–von Kármán force-constant model, while the coherent contribution $\mathcal{D}_2$ from the electron-phonon interaction is given by

$$\mathcal{D}_2(\kappa\alpha,\kappa'\beta,\mathbf{q})=-\frac{1}{N}\sum_{\mathbf{k},\mu,\nu}\frac{f_{\mathbf{k},\mu}-f_{\mathbf{k}+\mathbf{q},\nu}}{\varepsilon_{\mathbf{k},\mu}-\varepsilon_{\mathbf{k}+\mathbf{q},\nu}}\times g^{\kappa\alpha}_{\mathbf{k},\mu,\mathbf{k}+\mathbf{q},\nu}\, g^{\kappa'\beta}_{\mathbf{k}+\mathbf{q},\nu,\mathbf{k},\mu}\ , \tag{1}$$

in which κ is a site index, α a Cartesian coordinate, μ a band index, and g the matrix element of the electron-phonon interaction (the explicit form of g for a lattice with a basis is given in Ref. 11).

The phonon spectrum which arises from $\mathcal{D}_1$ is obtained by fixing the slopes to match the neutron-scattering results of Hallman and Brockhouse for fcc $Fe_{0.7}Ni_{0.3}$ at 296 K.[24] The calculated phonon dispersion curves are shown in Fig. 6 for $\mathbf{q}$ along the [110] and along the [111] direction. For the first case we find that the LA and the TA_2 branches are much affected by the nesting, whereas the TA_1 branch is not influenced at all. Fermi-surface nesting is really the source of this softening. This is obvious from the dispersion curves along [111]. There is no nesting for this direction, therefore, the TA_2 branch does not show any softening effects.

The generalized susceptibility which enters $\mathcal{D}_2$, was evaluated by using FSM band-structure data and the tetrahedron method of Rath and Freeman,[25] whereas the electron-phonon matrix elements were approximated by $g(q/q_{\max})$. A self-consistent evaluation of the electron-phonon matrix elements is still needed, since it will help to clarify why the extrapolated sound velocities from neutron-scattering data taken above the Curie temperature agree with the ultrasonic velocities, while there is a marked difference below T_C. Up to now, this difference has been attributed to magnetoelastic excitations, which are created during the acoustic measurements, while neutrons seem to couple less strongly to these excitations. But this is speculative. Nonetheless, a first-principle evaluation of the electron-phonon matrix elements for small

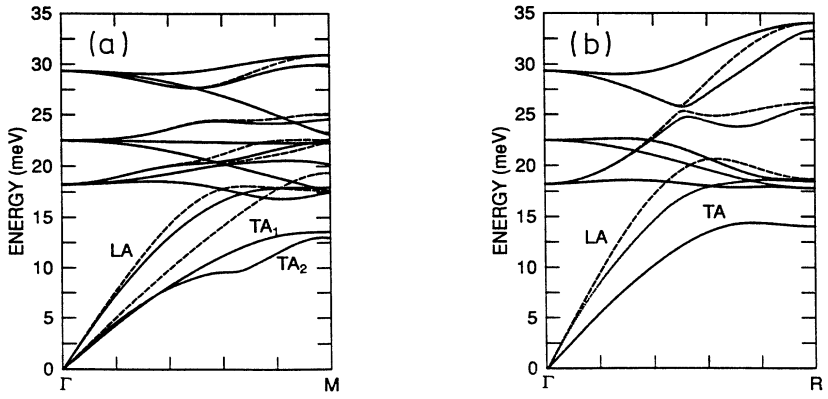

FIG. 6. Calculated phonon dispersion curves of fcc Fe_3Ni (a) along the [110] direction, and (b) along the [111] direction. The large background of the susceptibility was subtracted before the renormalized dispersion curves (solid lines) were evaluated with an electron-phonon coupling constant $g=0.574$ eV/Å.

q would show whether there is additional softening in the magnetic phase due to a particular strong magnetoelastic coupling. Recent measurements of the ultrasonic velocities in the Invar $Fe_{0.72}Pt_{0.28}$ seem to prove that the negative thermal expansion in the ferromagnetic phase at low temperatures is directly associated with the longitudinal-acoustic-mode softening caused by magnetoelastic interactions.[26]

Because all calculations have been performed for ordered Fe_3Ni, optical phonon branches are also obtained. Due to the small mass difference between iron and nickel, and due to disorder, the gap between acoustic and optical branches will be smeared out. This explains why the experimental spectrum only shows acoustic-like phonon branches.[24] Although the experimental curves were obtained at 296 K, which is very close to the onset of the $\gamma \rightarrow \alpha$ transition at 273 K, the curves do not show any kind of softening effects. This does not mean that the Kohn anomaly, which we predict for the case of Fe_3Ni, is completely absent. Our calculations are zero-temperature calculations, and it may be that disorder and high temperatures can mask the softening of phonon branches. On the other hand, we believe that in the case of disorder, we also will have a strongly enhanced susceptibility, which could be the electronic origin of large anharmonicity. For clarification further experimental results and calculations, which include disorder, are needed.

IV. FSM-GL THEORY OF THE MARTENSITIC TRANSITION IN $Fe_{1-x}Ni_x$

In order to study the stability of magnetic and structural phases it is quite helpful to use an extended Ginzburg-Landau expansion together with the FSM procedure. In the case of Invar, this allowed us to evaluate the temperature evolution of the binding surface, and to discuss the temperature variation of thermal expansion, magnetic susceptibility, compressibility, specific heat, etc.[6,27] For the case of Fe_3Ni the optimal GL energy corresponds to an expansion in terms of two magnetization fields, one for Fe and one for Ni. In addition we must add a constraint which fixes the average magnetic moment per atom.[6] This leads to

$$\mathcal{H}=\frac{1}{V}\int d^3r\left[\tfrac{1}{2}B\omega^2+\gamma\omega^3+\delta\omega^4+a_1(\omega_1-\omega)\mathbf{m}_1^2(\mathbf{r})+b_1\mathbf{m}_1^4(\mathbf{r})+c_1\mathbf{m}_1^6(\mathbf{r})+d_1\mathbf{m}_1^8(\mathbf{r})+a_2(\omega_2-\omega)\mathbf{m}_2^2(\mathbf{r})+b_2\mathbf{m}_2^4(\mathbf{r})\right.$$
$$\left.+c_2\mathbf{m}_2^6(\mathbf{r})+d_2\mathbf{m}_2^8(\mathbf{r})+J_1\mathbf{m}_1^2(\mathbf{r})\mathbf{m}_2^2(\mathbf{r})+J_2\mathbf{m}_1(\mathbf{r})\mathbf{m}_2^3(\mathbf{r})+J_3\mathbf{m}_1^3(\mathbf{r})\mathbf{m}_2(\mathbf{r})\right], \tag{2}$$

$$\mathbf{M}(\mathbf{r})=\tfrac{1}{4}[3\mathbf{m}_1(\mathbf{r})+\mathbf{m}_2(\mathbf{r})]\ . \tag{3}$$

Here, m_1 is the Fe and m_2 the Ni moment; $\omega=[V(T)-V_0]/V_0$ is the relative volume, V_0 a reference volume, B the bulk modulus, and $\omega_{1,2}$ are critical volumina introduced for convenience. Gradient terms have been left out, since we consider in this paper only the zero-temperature case.

Calculations have been done according to the FSM method. We fix the average magnetic moment M per atom and determine the individual moments self-consistently. In the case of Fe_3Ni this has led to a binding surface with coexisting LM and HM states close to a magnetovolume instability. GL parameters have been obtained from a fit to the original FSM first-principles binding surface. The discussion in Ref. 6 has shown that the binding surface of Fe_3Ni can be visualized as a superposition of the binding surfaces of fcc Fe and fcc Ni.

For a discussion of structural changes, we must include a series expansion in the Lagrangian strain tensor components η_{ij} for the cubic $m3m$ Laue group.[28] In order to describe the fcc$\rightarrow$bcc transition in terms of tetragonal or shear deformations, it is better to reformulate this expansion in terms of six linear combinations of the η_{ij} (i.e., symmetry adapted strain tensor combinations), which form the base of the irreducible representations. From these six combinations we use for simplicity only

$$\eta_0=\eta_{11}+\eta_{22}+\eta_{33}\ ,$$
$$\eta_1=(\eta_{33}-\eta_{22}-\eta_{11})/\sqrt{3}\ , \tag{4}$$
$$\eta_2=\eta_{11}-\eta_{22}\ ,$$

where η_0 has A symmetry and is identical with ω in (2), and η_1 and η_2 have both E symmetry and correspond to the tetragonal deformation $(c/a-1)$ and to the shear deformation, respectively. The final form of the Landau expansion including lowest-order coupling to the magnetization field is then of the form

$$\mathcal{H}[\mathbf{M},\eta_0,\eta_1,\eta_2]=\mathcal{H}[\mathbf{M}]+\frac{1}{V}\int d^3r\left[\tfrac{1}{6}(C_{11}+2C_{12})\eta_0^2+\tfrac{1}{54}(C_{111}+6C_{112}+2C_{123})\eta_0^3\right.$$
$$+\tfrac{1}{648}(C_{1111}+8C_{1112}+6C_{1122}+12C_{1123})\eta_0^4+\tfrac{1}{12}(C_{111}-C_{123})\eta_0(\eta_1^2+\eta_2^2)$$
$$+\tfrac{1}{4}(C_{11}-C_{12})(\eta_1^2+\eta_2^2)+(1/24\sqrt{3})(C_{111}-3C_{112}+2C_{123})\eta_1(\eta_1^2-3\eta_2^2)$$
$$+\tfrac{1}{3}B_1\eta_0\mathbf{M}^2-(1/2\sqrt{3})B_1\eta_1(M_x^2+M_y^2-2M_z^2)+\tfrac{1}{2}B_1\eta_2(M_x^2-M_y^2)$$
$$\left.+K_1(M_x^2M_y^2+M_y^2M_z^2+M_z^2M_x^2)\right], \tag{5}$$

where $\mathbf{M}, \eta_0, \eta_1, \eta_2$, are assumed to depend on $\mathbf{r}$, so that at finite temperatures these parameters can be decomposed into homogeneous and fluctuating contributions. These fluctuation terms can be used to calculate the magnetoelastic excitation spectrum[29] or the softening of phonon modes due to static deformations.[30,31] A more detailed account of this finite-temperature theory will be presented elsewhere. Here we consider only zero temperature.

The Landau expansion shows that in principle one would have to treat tetragonal and shear deformations on an equal footing, since the Landau coefficients for both strains are equally large. However, this makes a fit to first-principles FSM data difficult, since FSM total-energy calculations have only been done for deformation along the Bain path, which corresponds to tetragonal distortions. Therefore, we will neglect contributions from shear deformations. Furthermore, Fig. 2(a) shows that the derivative of the total energy, $\partial E/\partial \eta_1$, with respect to tetragonal distortions vanishes in the fcc and bcc ground state. This implies that the term which describes the linear coupling of M_α^2 to η_1 must be small or vanishes, and that a quadratic coupling of the order parameter to the strain field must be taken into account. In order to get a first impression of the martensitic transition along the Bain path, we neglect the LM state and use the following expansion in powers of the average magnetic moment per atom and strain fields:

$$\mathcal{H}[\mathbf{M},\eta_0,\eta_1]=+\frac{1}{V}\int d^3r[(B/2)\eta_0^2+\gamma\eta_0^3+\delta\eta_0^4+(a_1+a_2\eta_0+a_3\eta_0^2+D\eta_1^2)\mathbf{M}^2+(b+b_2\eta_0+D'\eta_1^2)\mathbf{M}^4$$
$$+c\mathbf{M}^6+d\mathbf{M}^8+A\eta_1^2+B\eta_1^3+B'\eta_0\eta_1^2+C\eta_1^4+C'\eta_0^2\eta_1^2]\ . \tag{6}$$

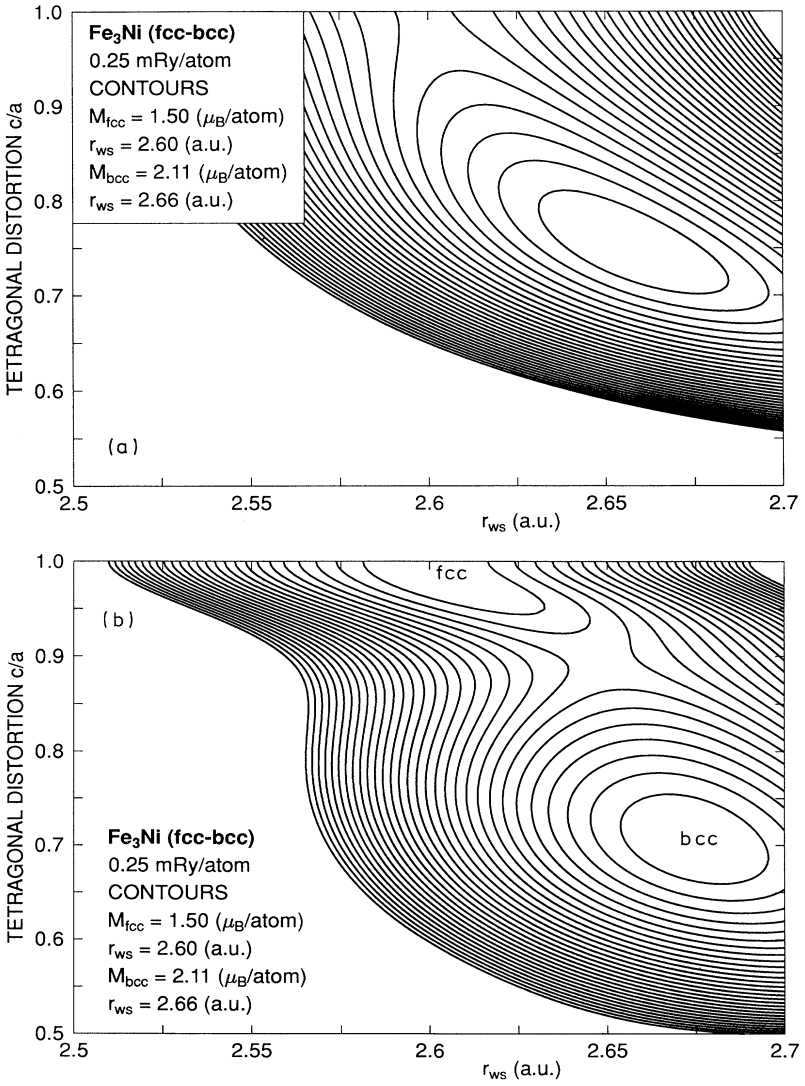

FIG. 7. The martensite binding surface of Fe_3Ni (a) for constant magnetization $M = 2.11\mu_B$/atom, and (b) for the correct magnetization along the Bain path shown in Fig. 2(b). Note that only in case (b) two local minima [corresponding to the fcc phase ($c/a=1$) and to the bcc phase ($c/a=\sqrt{2}/2$)] are obtained.

TABLE I. Coefficients of the fixed-spin-moment Ginzburg-Landau theory.

B	γ	δ	a_1	a_2	a_3	D	b	b_2
1193.112	−445.963	0	−0.975	−28.699	0	−51.95	0.415	0
D'	c	d	A	B	B'	C	C'	
5.631	0.049	0	33.773	−286.879	−271.653	0	11.2	

Values for the coefficients of this simple Landau expansion can be obtained by a fit to FSM total energies for the Bain transformation. They are listed in Table I. The resulting binding surface of energy contour lines in the $(c/a, r_{WS})$ plane is shown in Figs. 7(a) and 7(b) for two different cases. In case (a) we show the projection of the binding surface for constant $M=2.11\mu_B$/atom. This projection shows that the surface has only one local minimum corresponding to the bcc phase, and a saddle point corresponding to the fcc phase. For any constant M one only gets one local minimum. Also the resulting slopes at $c/a=1$ are not finite as one would expect. The reason for this behavior is obvious from Fig. 2(b) and from the Landau expansion. Figure 2(b) shows that the moment is not constant or does not vary linearly for the Bain path, but exhibits a minimum at $c/a=1$ and at a maximum at $c/a=\sqrt{2}/2$. With respect to the Landau expansion, there is only a fourth-order term of η_1, which is insufficient to obtain a second minimum on the binding surface due to the expansion alone (a second minimum would require an expansion up to eighth order). In order to solve this problem, we have added the constraint to the Landau expansion, that the magnetic moment varies according to Fig. 2(b) along the Bain path. This can be done very accurately by imposing for the variation of the moment the condition

$$M=2.11-57\,649.242(c/a-\sqrt{2}/2)^8 \times[1-9.652\,309\sin^2(c/a-\sqrt{2}/2)]\ . \quad (7)$$

The resulting surface in Fig. 7(b) has now two local minima corresponding to the fcc and the bcc structure. The energy difference between the fcc and bcc minima is of the correct order, while the energy barrier around the fcc minimum is a bit too large (0.5 mRy).

We believe that this Landau expansion will give a qualitatively correct description of Fe_3Ni also at finite temperatures. Fluctuations of strain and magnetization fields will destabilize the ferromagnetic bcc phase and will lead at high temperatures to a nonmagnetic fcc phase.

V. CONCLUSIONS

The present work is a continuation of the zero-temperature calculations of the physical properties of Fe_3Ni. In Ref. 6 we have shown that Invar properties arise from the particular position of the Invar Fermi level. At zero temperature many electrons occupy flat bands of strongly antibonding character. With increasing temperature these states can be depopulated resulting in a lattice contraction and a rapid decrease of the magnetic moment. We have explained that this is a cooperative effect and that a typical excitation energy of 1 mRy is involved.

In the present paper we have shown that there is another excitation energy connected with the structural transformation from fcc to bcc. Indeed, at zero temperature fcc Fe_3Ni is unstable with respect to small tetragonal or shear deformations. We have found that the bcc phase is about 1.75 mRy lower in energy than the fcc phase. Although the absolute values of these two excitation energies may change (for example, in a full potential calculation), there seems to emerge a unified picture for both the formation of Invar and the formation of martensite.

The magic electron numbers for ferromagnetic and antiferromagnetic Invar are connected with the specific position of the Fermi level at the crossing of antibonding majority-spin and nonbonding minority-spin states *in the antibonding region.* While this might also happen in elemental systems such as fcc iron for appropriate values of the Wigner-Seitz radius, there is another feature that appears in the intermetallic compound $Fe_{0.65}Ni_{0.35}$ due to the presence of Ni, which stabilizes the high-volume high-moment fcc ground state. The presence of Ni is also responsible for the appearance of a second minimum, the LM ground state. FSM calculations show that coexisting HM and LM states are still present for composition Fe_3Ni.

On the other hand, nickel causes a lattice softening which for a Ni concentration below some critical value leads to the observed martensitic transformation. Below this critical concentration of Ni, there are not enough d electrons in the strongly antibonding states to maintain the high-volume high-moment state. These zero-temperature findings agree with the observation that Fe_3Ni undergoes a structural transformation from the more-closed-packed structure (fcc) at high temperatures to a less-closed-packed ferromagnetic structure (bcc) at low temperatures.

Furthermore, we have shown that as in the case of Invar, the martensitic transition can be understood on the basis of a Ginzburg-Landau theory which relies on FSM results. The martensite binding-surface obtained with the help of an extended version of this FSM-GL formulation displays two local minima, which correspond to the bcc and the fcc phase, respectively. Further calculations are

needed to elucidate the finite-temperature behavior. We expect from a proper calculation based on a spin and strain fluctuation theory, that for Fe_3Ni, the local bcc and fcc minima, as well as the local minima corresponding to the HM and LM states, will merge together at the martensitic transition.

ACKNOWLEDGMENTS

One of us (P.E.) is grateful to E. F. Wassermann for very useful discussions. S.G.M. would like to thank the SFB 166 for financial support during his stay at Duisburg.

[1] *ISOMES'89,* Proceedings of the International Symposium on Magnetoelasticity and Electronic Structure of Transition Metals, Alloys, and Films, edited by E. F. Wassermann, K. Usadel, and D. Wagner [Physica B **161** (1989)]; E. F. Wassermann, Phys. Scr. **T25**, 209 (1989); in *Ferromagnetic Materials,* edited by K. H. J. Buschow and E. P. Wohlfarth (Elsevier, Amsterdam, 1990), p. 237; J. Magn. Magn. Mater. **100**, 346 (1991); Europhys. News **22**, 150 (1991).

[2] V. L. Moruzzi, Phys. Rev. B **41**, 6939 (1990).

[3] M. Podgorny, Acta Phys. Pol. A **78**, 941 (1990).

[4] P. Mohn, K. Schwarz, and D. Wagner, Phys. Rev. B **43**, 3318 (1991).

[5] V. L. Moruzzi, Solid State Commun. **83**, 739 (1992).

[6] P. Entel, E. Hoffmann, P. Mohn, K. Schwarz, and V. L. Moruzzi, Phys. Rev. B (to be published).

[7] E. C. Bain, Trans. AIME **70**, 25 (1924).

[8] F. E. Fujita, S. Nasu, and H. Adachi, J. Phys. C **4**, 103 (1982).

[9] J. A. Krumhansl, in *Nonlinearity in Condensed Matter,* edited by A. R. Bishop, J. K. Campbell, P. Kumar, and S. E. Trulinger (Springer, Berlin, 1986), p. 255.

[10] Y.-Y. Ye, Y. Chen, K.-M. Ho, and B. N. Harmon, Phys. Rev. Lett. **58**, 1769 (1987).

[11] G. L. Zhao and B. N. Harmon, Phys. Rev. B **45**, 2818 (1992).

[12] G.-L. Zhao, T. C. Leung, B. N. Harmon, M. Keil, M. Müllner, and W. Weber, Phys. Rev. **40**, 7999 (1989).

[13] R. J. Gooding and J. A. Krumhansl, Phys. Rev. B **39**, 1535 (1989).

[14] Per-Anker Lindgård and O. G. Mouritsen, Phys. Rev. Lett. **57**, 2458 (1986).

[15] S. Kartha, T. Kastan, J. A. Krumhansl, and J. P. Sethna, Phys. Rev. Lett. **67**, 3630 (1991).

[16] A. R. Williams, V. L. Moruzzi, J. Kübler, and K. Schwarz, Bull. Am. Phys. Soc. **29**, 278 (1984).

[17] K. Schwarz and P. Mohn, J. Phys. F **14**, L129 (1984).

[18] A. R. Williams, J. Kübler, and C. D. Gelatt, Jr., Phys. Rev. B **19**, 6094 (1979).

[19] H. Ebert (private communication).

[20] G. L. Krasko and G. B. Olson, Phys. Rev. B **40**, 11 536 (1989).

[21] J. Kaspar and D. R. Salahub, Phys. Rev. Lett. **47**, 54 (1981).

[22] V. L. Moruzzi, E. Hoffmann, K. Schwarz, and P. Mohn (unpublished).

[23] C. M. Varma and W. Weber, Phys. Rev. Lett. **39**, 1094 (1977); Phys. Rev. B **19**, 6142 (1979).

[24] E. D. Hallman and B. N. Brockhouse, Can. J. Phys. **47**, 1117 (1969).

[25] J. Rath and A. J. Freeman, Phys. Rev. B **11**, 2109 (1975).

[26] Ll. Mañosa, G. A. Saunders, H. Rahdi, U. Kuwald, J. Pelzl, and H. Bach, Phys. Rev. B **45**, 2224 (1992).

[27] M. Schröter, thesis, Duisburg, 1992.

[28] M. P. Brassington and G. A. Saunders, Phys. Rev. Lett. **48**, 159 (1982).

[29] V. G. Bar'yakhtar and E. A. Turov, in *Spin Waves and Magnetic Excitations 2,* edited by A. S. Borovik-Romanov and S. K. Sinha (Elsevier, Amsterdam, 1988), p. 333.

[30] E. Pytte, Phys. Rev. B **3**, 3503 (1971).

[31] P. M. Levy, J. Phys. C **6**, 3545 (1973).